Differential Optical Absorption Spectroscopy (DOAS) and Differential Absorption Lidar (DIAL) applied to atmospheric mercury monitoring.

Diploma paper

by

Joachim Kamme

Lund Reports on Atomic Physics, LRAP-65.

October 1986

Introduction

This work deals with optical monitoring of atmospheric atomic mercury. Two different techniques have been used. Firstly, the differential optical absorption technique (DOAS) was employed in a field measurement at a refuse disposal site. The system set-up and results from the measurement are presented in this paper. Secondly, the Lidar system here in Lund has been improved in order to reach an operational status for DIAL monitoring of atmospheric mercury. A tuning device for small and precise tunings of the laser wavelength is presented. Initial measurements have been made,and the results are included in this paper. Later on further tests will be made using a, specially designed absorption cell, which is also described here.

I wish to thank my advisors and cooperators Hans Edner, Bo Galle, Anders Sunesson, Sune Svanberg, Leif Une'us and Svante Wallin. Rolf Olofsson, Göran Werner and John Bergin have converted my drawings into mechanical constructions. I am also grateful to Åke Bergqvist and Bertil Hermansson for helping me in designing the electronic circuits.

Lund, October 1986.

Joachim Kamme

1. Why is mercury an interesting substance?

1:1 Mercury, an environmental threat

Mercury is a pollutant which has received appreciable attention during recent years, since the substance has proved to be a major environmental threat.

Besides atomic vapour, a number of different compounds are present in the environment, both organic and inorganic ones, with different toxicological properties. Atomic vapour is the main constituent of the mercury present in the atmosphere. It occurs all over the earth at a low concentration, 0.25-0.75 ppt (parts per trillion) (equivalent to 2-6 ng/m^3), which stems from a natural background (75%) and anthropogenic emissions (25%)[1]. But the most interesting form of mercury, concerning health and the environment, is the organic compound methylmercury (CH_3Hg). Methylmercury is produced through biological processes in the water and mud in lakes. The compound is extremely stable in biological systems and has a pronounced tendency to accumulate in the biological nutritoinal chain, therefore higher standing predators are liable to be exposed to high concentrations of this compound.

In Sweden the impact of mercury on the environment was revealed when certain families of fish-preying birds proved to be on the limit of extinction. Methylmercury was responsible for this, and it was found in such concentrations in the nutritoinal chain that the birds' eggs were damaged. Abnormal amounts of mercury were found in fish and sea-birds, and even in landanimals extreme concentrations were found. Then the problem concerned both land and water. Agriculture had for years used fertilizing substancies containing mercury and industry had released tons through drains and chimneys. Today the outlets have been greatly reduced, fertilizers containing mercury are forbidden, but a large number of Swedish lakes are still blacklisted because the concentrations of methylmerury in fish exceed the limit where it is considered to be harmful to human beings.

Mercury is believed to perform a cyclic motion, in which it is continously deposited and re-emitted from land and water [1].
Increased concentrations of mercury in lakes may sometimes be the result of local anthropogenic emissions, e.g from chloralkali-industries, but it is not always possible to connect it with a particular source. As discussed in [2] increased concentrations may also be obtained when the global cycle of mercury is disturbed by an environmental change like acidification. Acidification is believed to retard the process which converts methylmercury into elemental mercury, and thereby affect the re-emission of mercury from lakes, since it is the elemental form which

is re-emitted.

It is, indeed, of the greatest interest to assess the impact of anthropogenic mercury emissions and analyse the cyclic motion of mercury in our environment. For this reason methods capable of monitoring atmospheric mercury have to be developed. Optical techniques offer unique oppertunities for doing this.

1:2 Mercury vapour sensing for mineral exploration, and other fields of application

It has been known for a long time that vapour sensing techniques may be used for mineral exploration. Different vapours are often abundant in close association with different ores, due to degassing processes. By monitoring the abundance of a certain trace gas, deposits of e.g. ZnS have been localized [3]. Mercury seems to occur in association with a number of metals, e.g. gold. Greater or lesser amounts of mercury have been found in gold deposits depending on the age of the ore [4]. An optical range resolved technique capable of detecting and determining the location of a plume of mercury vapour is described in chap. 4. It is, indeed, well-suited to the task.

Volcanic activity is another area in which vapour sensing techniques may become applicable. As volcanoes are fed with new fresh magma, the amount of mercury released to the atmosphere increases, by monitoring this phenomenon it may be possible to forecast an eruption [5]. Fault zones have been mapped, after an earthquake in the Soviet Union, employing mercury sensing techniques [6]. Also, in localizing sources of geothermal energy, mercury vapour sensing techniques may be used as a track-finder [7].

2. Optical techniques, general considerations

A number of instrumental methods for monitoring mercury have been developed. See e.g. [8]. Certain optical methods though, have great advantages, since they possess the following properties: they are *in situ* methods, the sampling-time is relatively short and they are not point-measuring methods, which will compensate for possible local fluctuations.

Two techniques are described in this work, DOAS and DIAL. Since they work in different ways, the applications are different. Compared with DIAL, the DOAS technique is a more sensitive method. It is not limited by atmospheric scintillation effects, which limits DIAL, if two laser systems are not available. But it only provides path-averaged measurements, DIAL provides range-resolved. An appropriate application for DOAS, like the field measurement described in this work, is to measure the concentration of a trace substance, when good accuracy is desired, but the range does not have to be determined. Though, using tomographic techniques, some degree of range resolution may be obtained with DOAS. DIAL is employed when a trace substance is to be detected and localized or the concentration at a specific location assessed.

The difference in nature of the techniques is considerable. DIAL is a monostatic technique, i.e the transmitter and receiver are at the same location. DOAS, is bistatic in nature, the transmitter and receiver being located a distance away, which implies that only the volume of air between two points, can be analysed.

This is of course an advantage for the DIAL technique, but if the complexibility of the systems is considered, DOAS has the advantage of being not nearly as complex as a DIAL system.

When monitoring mercury by optical means, as in this work, the transition in the ultraviolet region at 253.65 nm ($6s^2\ ^1S_0$-$6s6p\ ^3P_1$) is employed. The width of this line is only about 0.05 Å and arises due to a number of naturally occurring isotopes, ^{196}Hg-^{204}Hg, and hyperfine structure, see Fig 1. This implies that a high spectral resolution is needed. The Doppler-broadening allows only some of the lines to be resolved.

A high spectral resolution is also needed since O_2 has a forbidden transition very close to 253.65 nm. This transition is very weak, but since the content of oxygen in the air is 18%, it will hamper any measurement if the resolution is not good enough.

The performance of an optical system is also determined by the broad-band transmission properties of the atmosphere. The scattering efficiency of molecules and particles (Rayleigh and Mie scattering respectively) is wavelength dependent, and increases with decreasing

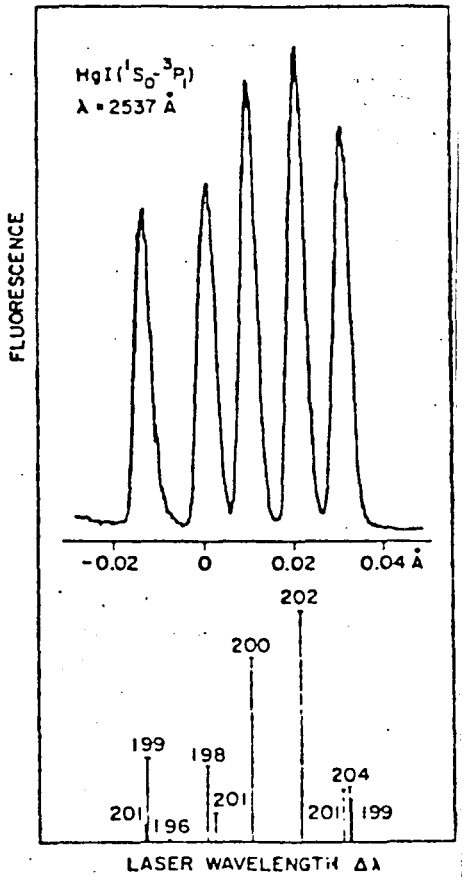

Fig. 1 The structure of the mercury $^1S_0$-$^3P_1$ transision, obtained with a laser linewidth less than 0.0008 Å. From [9].

wavelength. In the ultraviolet region the Mie scattering is very prominent, and will in DOAS, considerably affect the amount of light received from the transmitter. In DIAL the backscattered light from a transmitted pulse of laser light is detected, and in this case a limited range is expected due to the very intense Mie scattering.

3. Differential Optical Absorption Spectroscopy (DOAS) applied to atmospheric mercury monitoring

Differential Optical Absorption Spectroscopy (DOAS) is a relatively new technique, first described by Platt et al. [10], which has proved to be both a sensitive and uncomplicated technique. So far it has been applied on a number of trace substancies, e.g NO_2,SO_2 and hydrocarbons. Atmospheric mercury was monitored for the very first time in 1985 by the group in Lund [11]. The field measurement described in this paper is the third made in which DOAS is employed for atmospheric mercury monitoring.

Complete DOAS systems, extremely compact and easy to handle, are now commercially available. (Opsis AB, Lund, Sweden.)

3:1 Description of the DOAS technique

In DOAS a powerful broad-band lamp is employed, mounted a distance (100m-10km) away from the receiver system. The receiver system consists of receiver optics, a dispersive spectrometer, a scanning device, a detector (photomultiplier tube (PMT)), and a computer.

The receiver optics is made up of a telescope which collects the incoming light and focuses it onto the entrance slit of the monochromator, which disperses the spectrum. A minor segment of this spectrum is analysed by means of a scanning unit and a PMT. The scanning unit performs repetively fast scans through the spectrum, the pmt converts the optical signal into an electrical one, which is digitalized and stored in a minicomputer.

One scan is performed in about 10 ms, and with this rate of scanning, atmospheric scintillations are eliminated and the air will appear "frozen" since the frequency spectrum of atmospheric turbolence contains little energy above 10 Hz.

In one measurement several thousands of scans are integrated during several minutes. Noise effects and temporal signal variations will then be effectively surpressed.

Recorded spectra generally contain a broadband feature which stems from several sources. Lamp energy output varies with wavelength, mirrors used in the receiver optics have wavelength-dependent reflectivity and the scanning unit may also introduce such a broadband feature. In order to compensate for this structure a polynomial (1st-5th order) is least-squares fitted to the recorded spectrum. The polynomial will not be able to follow the sharp absorption features caused by the trace gases, and by
dividing the spectrum by this polynomial the broad-band featues are eliminated. The principle is illustrated in Fig. 2.

The differential absorption, i.e. the absorption at the resonance wavelength of the trace gas compared to the absorption at a wavelength slightly separated from this value, is given by the Beer-Lambert law

$$1-A=T=\exp(-\sigma n l)$$

where A is the absorption, T the transmittance, σ the differential cross-section, n the concentration of the trace gas and l the absorption path length.

Fig. 2 Principles of DOAS evaluation. The left plot shows the raw recorded spectrum and the fitted polynomial (3:rd degree). The right plot is the result after division.

The detection limit of a particular trace substance is determined by the strength of the absorption line, i.e. the differential cross-section, and the length of the lightpath used. In order to get a low detectionlimit, a long light path is desirable as a larger number of molecules, or atoms, are then active absorbers. But the intensity received from the lamp is inversely proportional to the length of the path due to the attenuation of the beam by atmospheric absorption and scattering. Hence an optimum path length exists for optimal sensitivity, and the value is determined by the

atmospheric broad-band absorption, Mie and Rayleigh scattering. These effects may be expressed in as an absorption length L_0. The intensity received then becomes $I_{received} \sim I_{source} \exp(-L/L_0)$, where L is the path length used. The signal-to-noise ratio may then be expressed as $S/N \sim L\exp(-L/2L_0)$, which, when optimized, gives an optimum path length of $L=2L_0$. (See [10]).

Losses of light may also be caused by geometrical factors. Since the telescope in the receiver system creates an image of the mirror used as reflector in the lamp at the entrance slit of the dispersive spectrometer, light is lost if the image is larger than the slit. But the size of the image decreases with the distance between lamp and receiver system, and it is, considering this effect, favourable to have a long light path.

3:2 Field measurements of atmospheric mercury at a refuse disposal site

Field measurements were carried out at a refuse disposal site in Alingsås 50 km north of Göteborg during three days in August 1986. Measurements were performed at two paths, see Fig. 3, the first 133 metres, the second 108 metres. The height above the ground was 0.3-0.7 m. These parts of the disposal site were 1.5 to 3 years old, and some parts were covered with a layer of earth. The weather conditions at the time of measurement were a daytime temperature of 20-25 ^{0}C, which fell during the night to 6-8 ^{0}C. Hardly any wind or any well defined wind-direction were present.

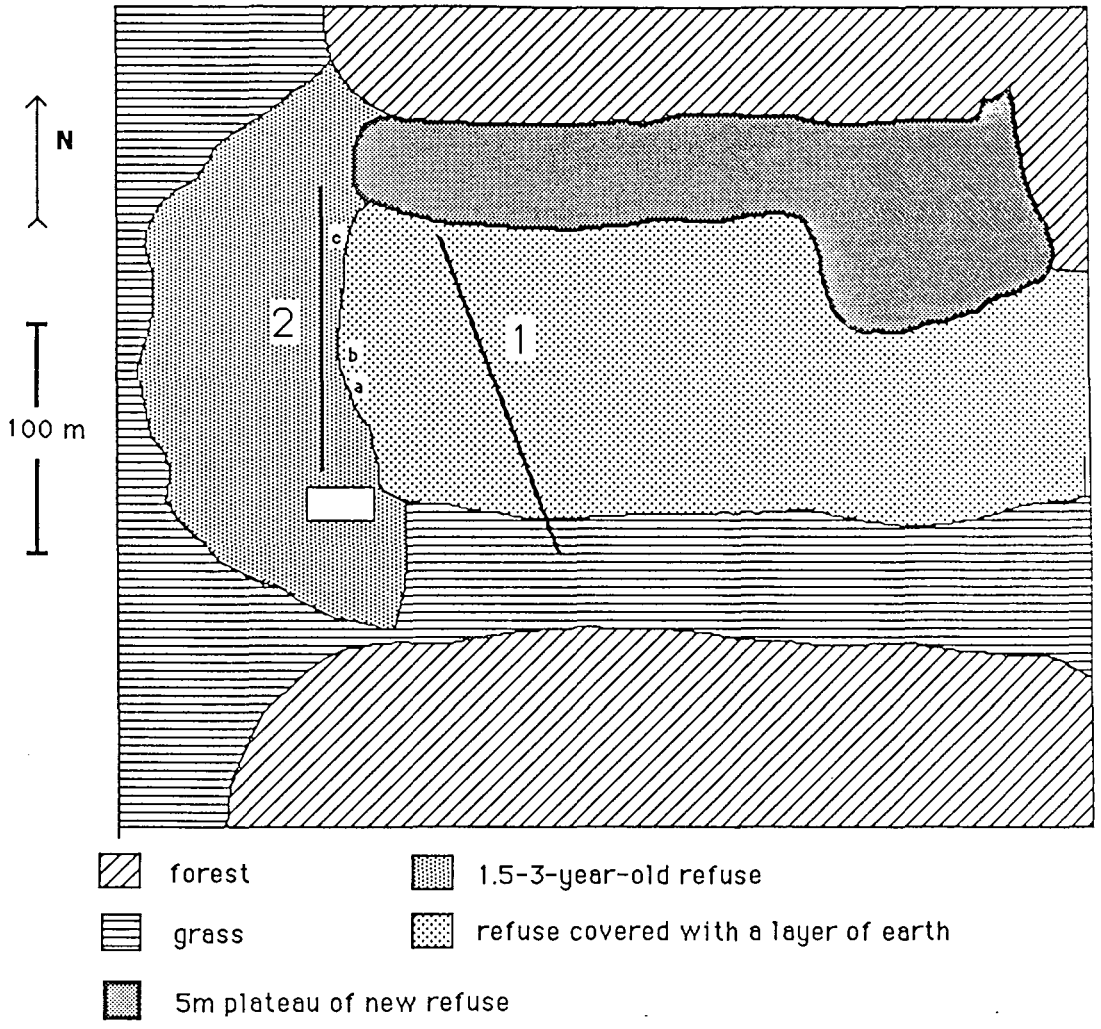

Fig. 3 Map of the disposal site. 1 and 2 are the measurement paths. a, b and c show the locations of the wind-recording equipment.

3:2:1. System description

A high pressure Xe arc-lamp was used as light source, put in focus of a concave mirror, f=25 cm, diameter 30 cm. This light source is further described in [12]. The receiver system was mounted in a Volkswagen van with a configuration as shown in Fig. 4.

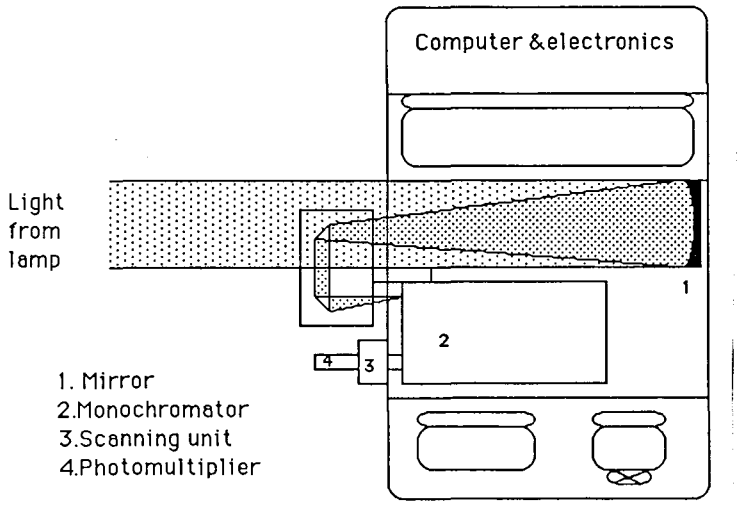

Fig. 4 Set-up of the DOAS equipment in the WV van.

A spherical mirror (f=2m, diam=.35m) focuses the incoming light. Two plane mirrors deflect the light onto the monochromator, which is a 1m monochromator in Czerny-Turner arrangement, including a holographic grating with 3000 r/mm. The monochromator runs in 2:nd order and grazing incidence, with a 5mm UG-5 filter put in front of the entrance slit in order to effectively suppress overlapping orders at the exit slit.

A rotating disk at the exit slit acts as the wavelength scanner. (Another approach is the rotating mirror, described in [11]). A number of slits, each 10 µm, are cut radially in the disk. As the disk rotates the slits pass through the spectrum, one at a time, and let a minor part through. See Fig. 5. An EMI 9558 PMT converts the optical signal into an electrical one.

A preamplifier converts the low-current signal from the PMT into a signal level of 1-10 V, which is digitalized and saved by the acqusition unit (described in [13]). 1024 samples are taken during the 12 ms period a slit is illuminated. Sampling of this unit is synchronized with the rotation of the disk using an infra-red light barrier and an electronic circuit, which produces a trigger pulse each time a slit in the
disk is a about to traverse the spectrum.

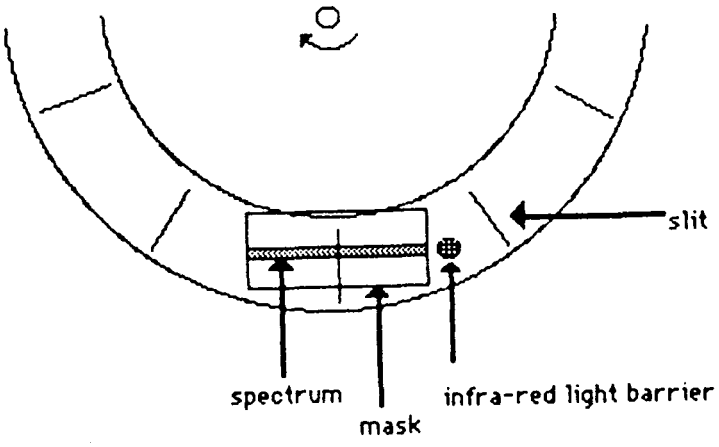

Fig. 5 The rotating disk.

In order not to hamper the spectral resolution the velocity of the rotating disk is kept constant within 0.1%. System steering and collection and processing of the recorded spectra are performed by a P80 microcomputer.

The spectral resolution obtained with this system was better than 0.1 Å. This order of resolving power is needed in order to resolve the mercury absorption line from a transition in O_2 [11].

3:2:2. Measurements

Measurements were performed for three days, 24 hours a day, with one measurement taking a quarter of an hour. In fifteen minutes 65535 scans of the spectrum are averaged. Interesting parameters such as wind velocity and wind direction, were continuously recorded at three locations, of which two were at a heigth of 1.5m above the ground, and the third at a heigth of 5 metres. (See Fig. 4.) The temperature was recorded every fifteen minutes.

Calibrations were made, using cells of saturated mercury vapour, 0.8 mm and 0.9 mm thick, placed in front of the entrance slit of the monochromator. Since the vapour pressure of mercury is strongly temperature dependent, the absorption due to the cells varied greatly from 6%, when both cells were used during daytime, to 0.5% at night. A plot of absorption vs. the introduced optical thickness of mercury is shown in Fig. 6.

The concentration of mercury at the measurement site proved to have a maximum of ~70 ng/m^3, which occurred during the daytime when there was no wind. At night the concentration decreased to a much lower value

~10 ng/m^3. The variation in mercury concentration during the three days of measurement is shown in Fig. 7.

An example of a measurement is shown in Fig. 8. From a raw recorded spectrum the noise level was assessed to be 0.5%, which, according to the calibration, gave a mercury detection limit of 10 ng/m^3.

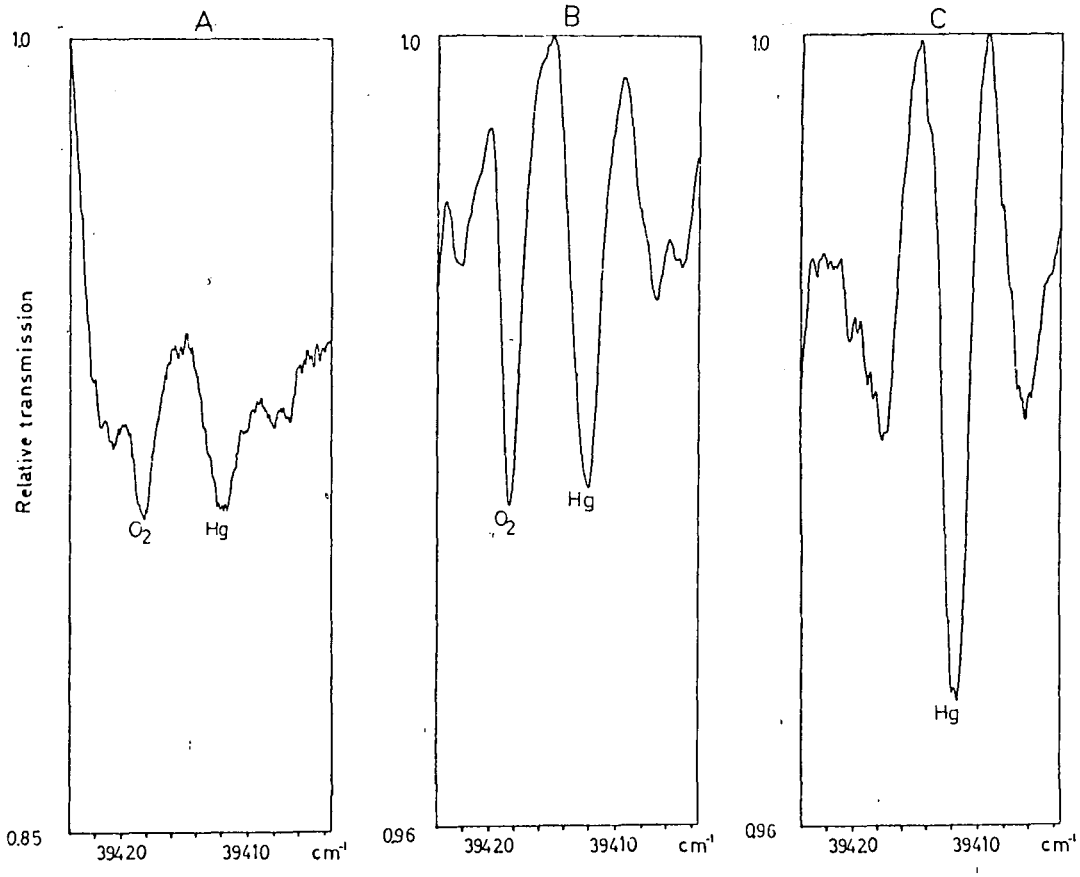

Fig. 8 Example of a measurement. A is the raw recorded spectrum, B the same spectrum divided by a 3:rd polynomial. Plot C is the result of a calibration measurement.

During the evaluation, one value of the differential cross-section has been used for all the measurements. Though this is somewhat erroneous, the sensitivity of the system was not kept constant since many adjustments had to be made due to instability of the system, the uncertainty in just one pair of calibrations proved to be too large. The differential cross-section, employing all calibrations except ones obviously affected by sunlight and ones made during cold hours at night, was computed to be $1.75*10^{-19}$ m^2.

The instability of the system, manifested as movements of the focusing

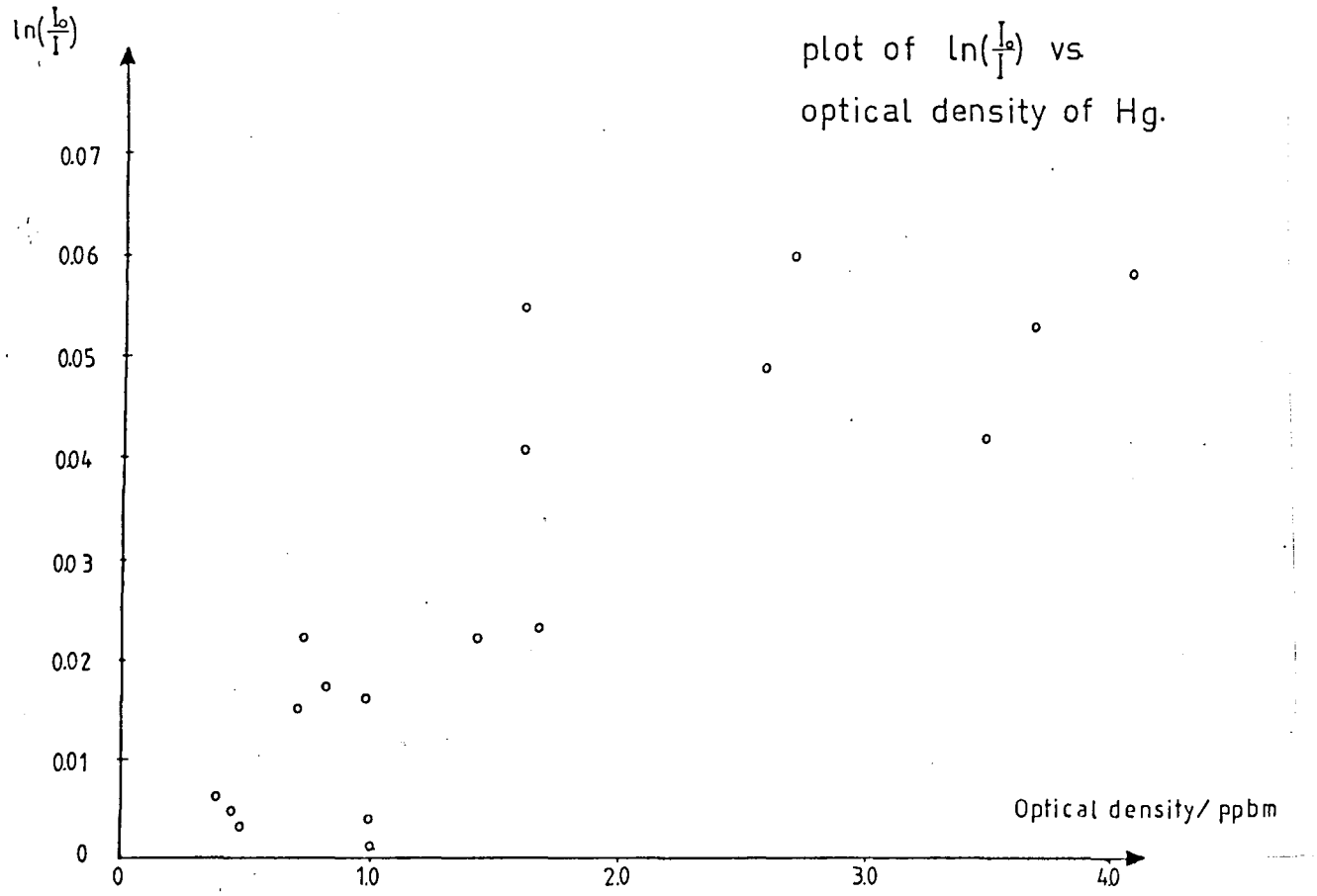

Fig. 6 Plot of $\ln(I_0/I)$ versus the optical density of mercury.
Compensation has been made for background absorption.

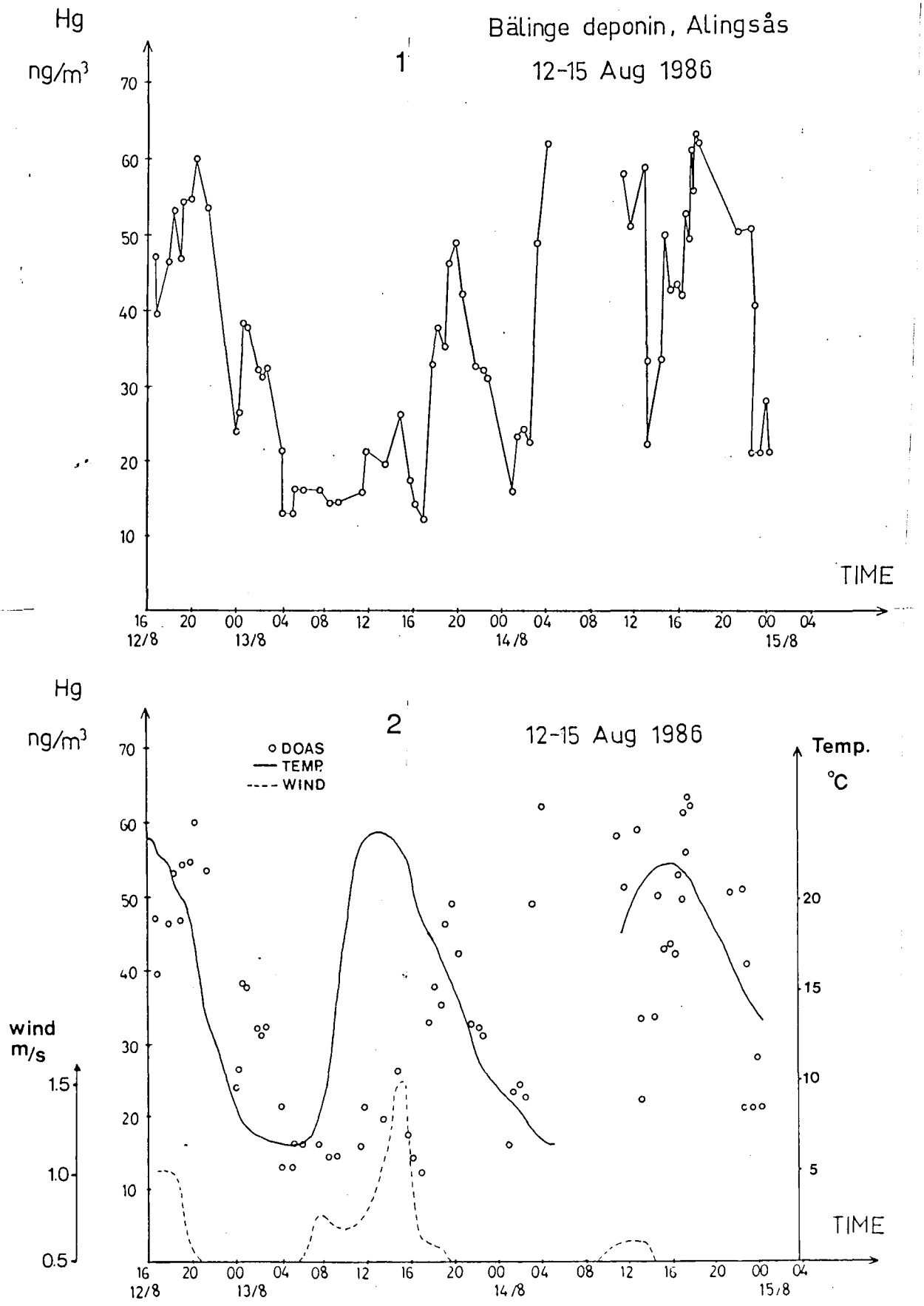

Fig. 7 Plot 1 shows the variation of the mercury concentration during the time of measurement. Plot 2 shows the temperature and wind velocity as a function of time, together with the mercury concentration.

beam, made the evaluation of the differential absorption due to mercury difficult. The result is dependent on which part of the spectrum that is used. Since the angle of incidence of the focusing light to the monochromator could not be kept constant, the position of of the mercury absorption line varied, and due to this phenomenon, the part of the spectrum over which the evaluation was made had to be changed a number of times during the evaluation.

Considering the error limits obtained, at least two sources have to be taken into account. Noise introduces an error of the order 4 ng/m^3. The calibration error, due to taking a mean value of the cross-section applied on all measurements, was estimated to be $0.25*10^{-19}$ m^2. This gives rise to a 15 per cent uncertainty in the evaluated concentration. Added together, the error in a measurement in which the evaluated concentration is 20 ng/m^3 is no more than 7 ng/m^3. Correspondingly for 40 ng/m^3 the figure is 10 ng/m^3, and for 60 ng/m^3 the figure is 13 ng/m^3.

3:2:3 Conclusions

As shown in [11], and in this field measurement, DOAS is a powerful method in atmospheric mercury monitoring. The simplicity and relatively low cost for a DOAS system are important features. A great advantage is that the same light source may be used for many trace substancies, it is even possible, in some cases, to monitor several trace gases at the same time. Although,the spectral resolution needed for mercury monitoring is quite high, most other applications need only intermediate spectral resolution.

Considering the system used, the stability was not satisfactory. An external telescope,positioned directly on the ground and connected with the monochromator with an optical fibre, would probably be more practical.

The results obtained clearly show that the concentration of mercury at this disposal site varies with the time of day. Peaks in the concentration are noted close to 20^{00} for all measurement days. The recordings of the wind velocity show that the velocity at this time decreases from a daytime (07^{00}- 20^{00}) value of 0.5-1 m/s to zero, and remains zero until the morning. By 20^{00} the sun is about to go down, but the ground is still warm, due to the radiation from the sun during the day. A plausible conclusion is that the emission of mercury goes on until the ground has cooled down. At 20^{00} the ground is warm, the emission of mercury large, and since there is no wind the mercury vapour remains at the site, which leads to high concentrations.

The concentrations recorded indicate that a desposal site of this kind

does not give any notable contribution to the mercury content of the atmosphere. The total emission of mercury from this disposal site was assessed to be less than 1 kg/year. The field measurement made before this, at Tagene disposal site [14], where ash from a refuse destruction plant was deposited, gave results more than an order of magnitude higher. The total amount of mercury emitted there was assessed to be ~10 kg/year.

4. Lidar (DIAL) applied to atmospheric mercury monitoring

Initial DIAL mercury measurements have been carried out here in Lund 1981 [15]. Since then a new lidar system has been constructed [17]. Some modifications and initial tests have been made aimed at an operational status for mercury measurements.

4:1 Basic Lidar approach

Lidar (acronym for Light Detection And Ranging) is based upon the following. A short pulse of laser light is transmitted into the the atmosphere. As it propagates, it is continously scattered by particles and molecules. The photons reaching the lidar system again, are collected and analysed time-resolved. (Fig. 9) The signal arriving at a time t corresponds to light from a stretch $c\tau_L/2$, where $c\tau_L$ is the length of the pulse, at a distance ct/2 from the source.

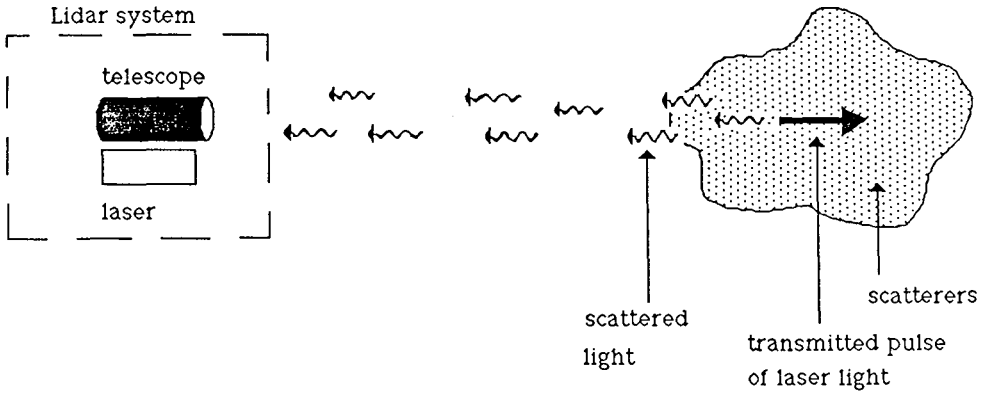

Fig. 9 The lidar principle

A mathematical analysis gives the power received as a function of the distance R. (See e.g. [16])

$$P(R)=C*P_L*\sigma_b*N(R)*A_0/R^2*c\tau_L/2*\exp(-2\int_0^R \sigma_\lambda n(R)+\sigma_a N(R)dR)$$

where C is a system constant

P_L is the laser pulse power

σ_b is the backscattering cross-section

N(R) the total number of scattering objects per unit volume

A_0/R^2 represents the acceptance solid angle of the receiver optics
$c\tau_L/2$ is the half length of the laser pulse
$\exp(-2\int\sigma_\lambda n(R)+\sigma_a N(R)dR)$ represents the attenuation due to absorption by the substance under investigation and particles
σ_λ is the cross-section for absorption by the trace gas
$n(R)$ is the trace gas concentration
σ_a is the cross-section for absorption by particles
$N(R)$ is the particle concentration

Basic lidar has a number of applications of which I will only mention a few. (See e.g. [16]) In the visible and infra-red parts of the spectrum, particles will generate most of the backscattered light. This can be used in order to map particle concentrations. Raman scattering can be employed to assess atmospheric temperature or humidity. Gaseous pollutants can be monitored with DIAL, which is to be treated in the next section. Another interesting lidar approach is the gas-correlation lidar, where a signal due to the pollutant is obtained by using the gas itself as an optical filter [18].

4:2 Differential Absorption Lidar (DIAL)

In DIAL a comparison between the lidar curves for two different wavelengths is made. One wavelength is tuned to an absorption line of the trace substance, the other slightly separated from this value. The on-signal will suffer from attenuation of the substance and the off not, and this is the only difference since the atmospheric transmission properties, excluding absorption by the trace gas, may be considered as constant if the difference between the on and off wavelengths is small. The general procedure is to divide the lidar curves for the on and off wavelengths. (See Fig.10) Logarithmation and differentiation will yield the concentration as a function of the distance. A simplified analysis gives

$$P_{ON}/P_{OFF}=\exp(-2\int_0^R\sigma_A n(R)dR)$$

σ_A is the differential cross-section of the molecule, $\sigma_A=\sigma_{ON}-\sigma_{OFF}$
A more rigorous treatment is found in [16].

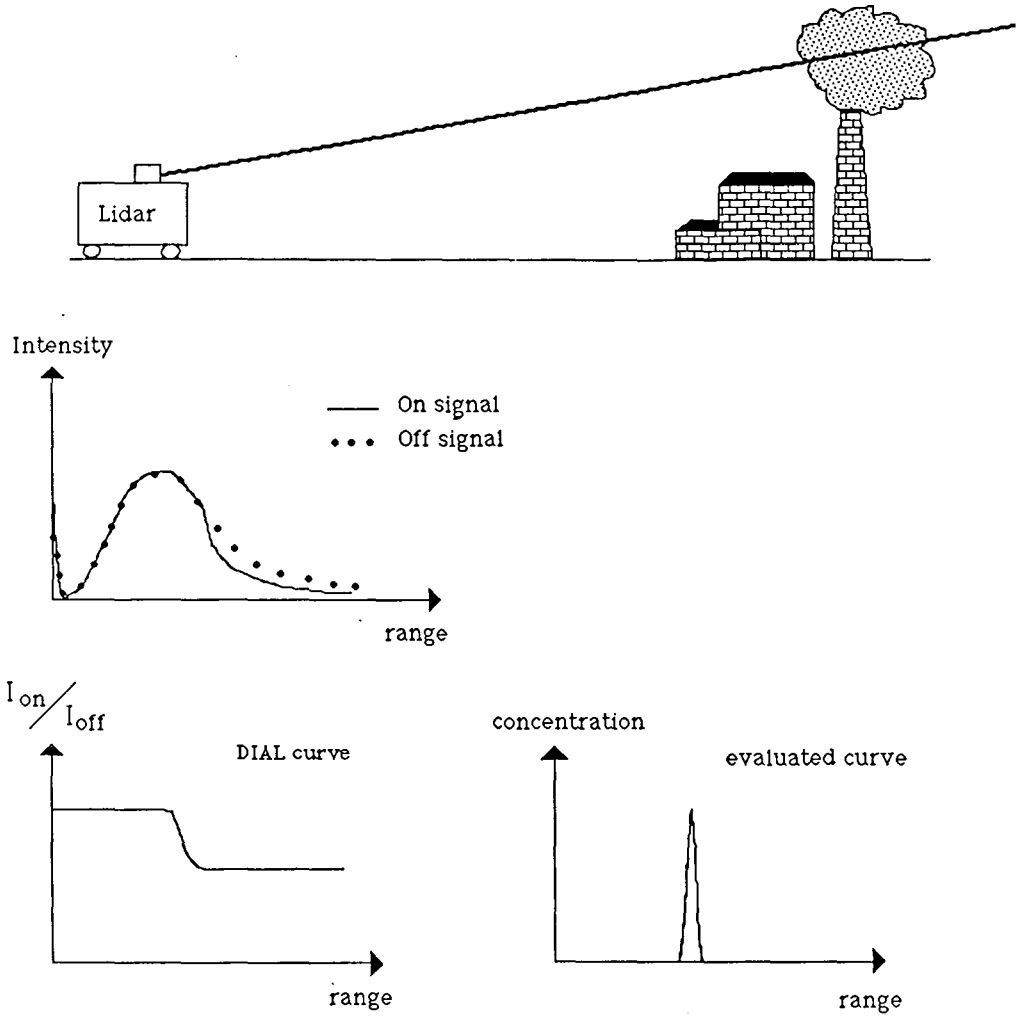

Fig. 10 Principles of DIAL

3. The Lidar van

The Lidar system is a mobile system constructed here at the Lund Institute of Technology [17]. It is the successor to the first system built at Chalmers University of Technology in Göteborg, described in [19]. Both have been financed by the Swedish National Environmental Protection Board and the Swedish Board For Space Activities.

The base platform is a van with a laboratory floor-area of 6.2.3 metres. (Fig. 11) A system description and a signal-flow diagram are provided in Figs. 12 and 13.

The YAG-laser is a Quanta-Ray DCR-1 producing 250 mJ pulses with a duration of 10 ns. The normal repetition frequncy is 10 Hz. The radiation from the YAG-laser, with a wavelength of 1.06 μm, is either doubled or trippled in a non-linear crystal. The light may then be continuously tuned by a Quanta-Ray PDL-1 dye-laser, consisting of a grating tuned oscillator with one or two amplifiers. After the dye-laser, necessary equipment, e.g. Raman-shifters and/or crystals, may be installed to reach the desired wavelength. Part of the beam is deflected by a beam-splitter, and directed towards the calibration equipment. A neon hollow-cathode lamp is used in order to make rough calibrations, employing the optogalvanic effect. A fine calibration is made by measuring the intensities of two beams, one of which has passed through a cell containing the gas of interest. Two prisms and a mirror deflect the beam through the telescope into the air. A beam-expander may be introduced in the beam path in order to protect the mirror from damage. The divergence of the beam is typically 1 mrad.

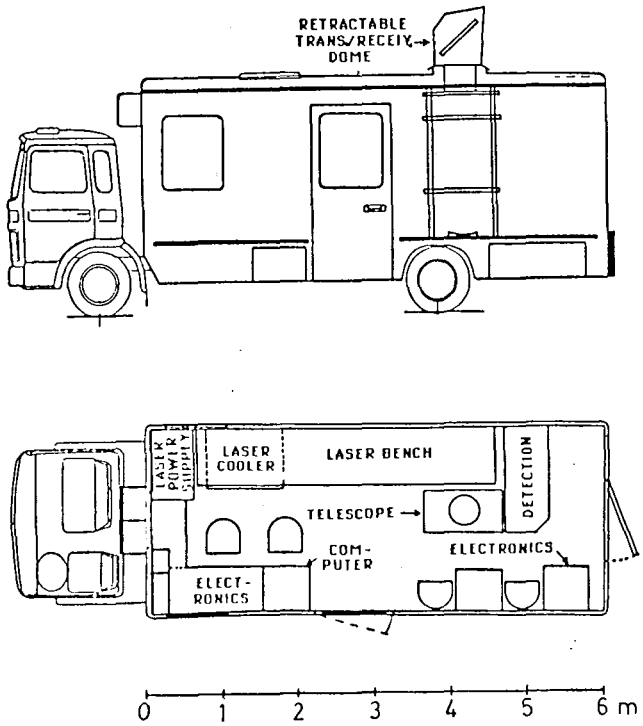

Fig. 11 The new lidar van. (From [17])

A Newtonian telescope collects the backscattered light. The focusing light passes through an iris which defines the telescope's field of view, and thereby the effective divergence of the laser beam. A quartz lens makes the light parallel, after which it passes through necessary optical filters which select the spectral region of interest. A photomultiplier, whose gain is modulated in order to compensate for the variation in the signal level, converts the optical signal into an electric one, which is digitalized and stored on a LeCroy transient-recorder. The computer, ITT-XT, collects the results through a GPIB interface.

In order to suppress the background radiation, besides optical filters, every tenth shot is blocked by a chopper. The signal then received is subtracted from the measurements.

Choice of wavelenghts, measurement direction and so on is performed through the computer.

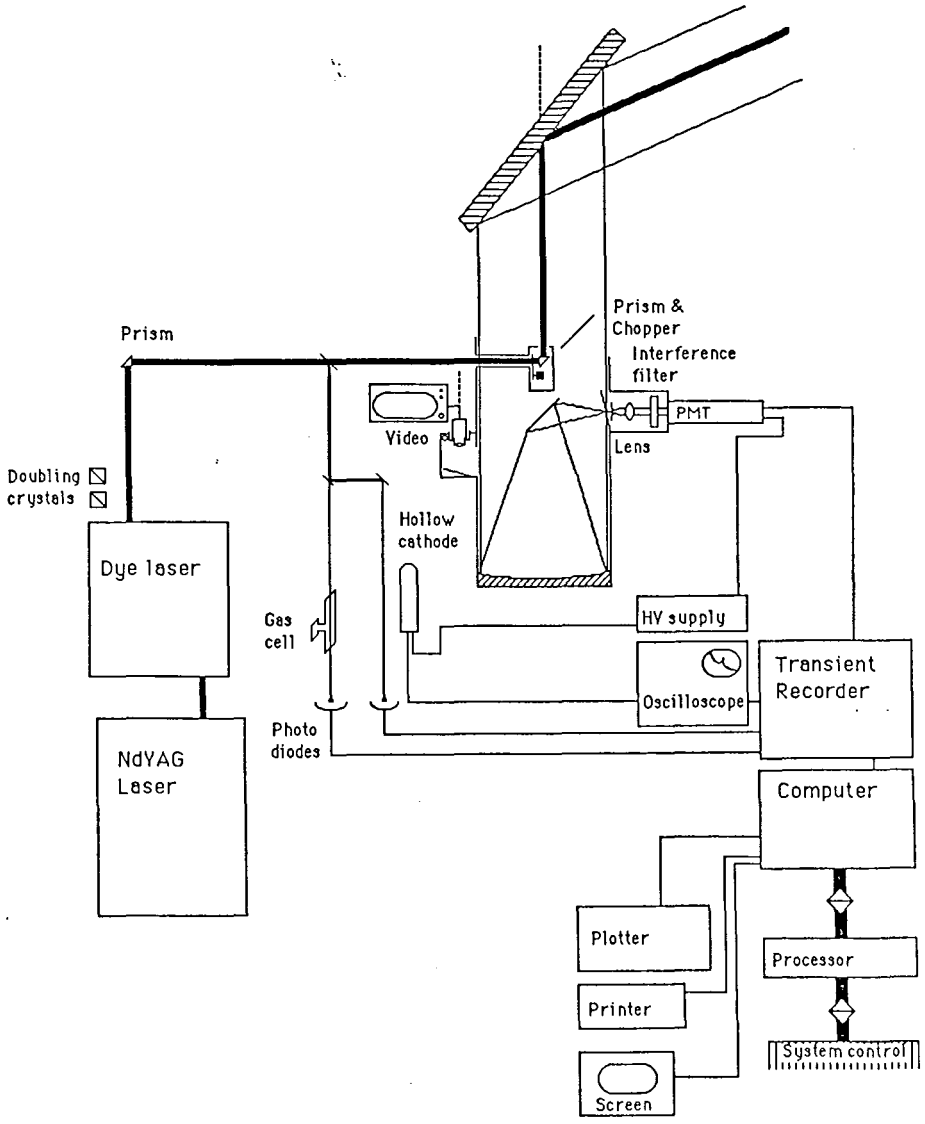

Fig. 12 Diagram of the lidar system. (From [17])

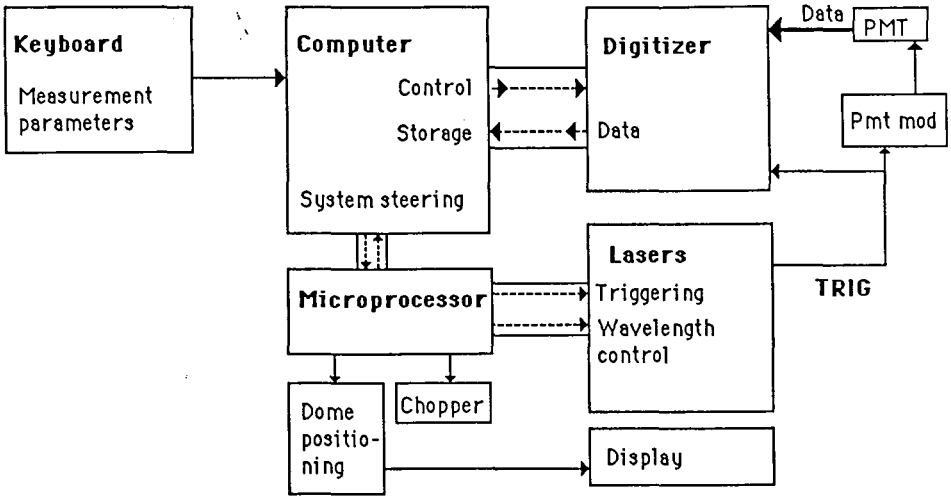

Measurement sequence

Directions etc are stored in the computer

The computer orders microprocessor to start, and it positions dome mirror

The computer waits for data in the digitizer

The microprocessor fires the laser and sets proper lambda

When the Q-switch pulse is released the laser trigs off digitizer and PMT modulation

Data collection

The computer receives data from the digitizer

A new cycle is started

Fig. 13 Diagram of the signal flow and a description of a measurement sequence. (From [17])

4:4. Mercury DIAL measurements

4:4:1. Set-up for mercury DIAL measurements

The use of ultraviolet light in the 2536 Å region suffers from a number of difficulties. The generation of the laser light, which is treated in the next section, becomes complicated, many steps are needed and the resulting pulse energy will be relatively low, which will lead to a limited range. Also, since the scattering efficiency of particles is very high in this region, the range will be reduced.

4:4:1:1 Generation of the mercury line at 253.65 nm

In order to reach the wavelength of interest additional equipment besides the YAG and the dye lasers is needed, since it is not possible to generate the wavelength directly. Several methods are available.

1. A coumarine dye in the dye laser with a subsequent KDP crystal is a conceivable configuration, but it has a number of drawbacks. The efficiency of coumarine dyes (≈10%) and the doubling efficiency in this region are poor (≈1%),and the resulting output power will be low.
2. Frequency mixing in a nonlinear crystal, using residual infra-red radiation from the YAG-laser and the dye laser loaded with rhodamine 6G (40% efficiency), will produce pulses with satisfactory energy but the resulting linewidth will be poor due to YAG laser linewidth.
3. The method which has proved to give the best results, so far, is stimulated Raman scattering in a cell with H_2-gas after a KDP-crystal. With a rhodamine-6G dye the dye-laser is tuned to 567.06 nm, a KDP-crystal doubles the energy to 283.54 nm and a Raman cell, with 8 atm. of H_2, shifts the light in discrete steps of 4155 cm^{-1}, of which the first anti-Stokes component will have the desired wavelength, 253.65 nm.

A Pellin-Broca prism acts as the dispersive element which allows for selection of the frequency to be transmitted. (Fig.14) The resulting pulse energy will be about 0.8 mJ, and 0.5 mJ of this will remain when the beam passes through the quartz window of the dome. Starting with 250 mJ from the YAG-laser, 50 mJ pulses leave the dye-laser, 20 mJ are converted by the KDP-crystal into doubled light, and finally 0.8 mJ will have the desired wavelength after the Raman shifter, a considerable reduction. The linewidth of the resulting radiation becomes about 0.20 Å, approximately four times greater than the width of the mercury absorption line, hence not all of the radiation will be available for absorption. It is possible to

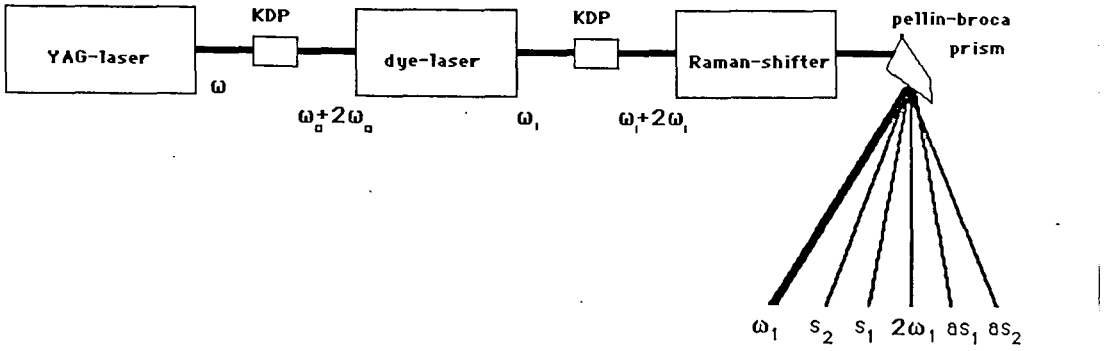

Fig. 14 Diagram of the laser set-up.

reduce the linewidth by introducing an etalon in the dye-laser, but the output power will be lowered to such an extent that the Raman shifter will work close to its threshhold value. It is, of course, desirable to keep the linewidth comparable to the width of the mercury line, but the loss of power due to the etalon causes the radiation to dissappear with only minute changes of adjustments.

The divergence of the resulting laser beam proved to be larger than expected, 1.2 mrad. This value was obtained by recording the echo when the beam was directed through a circular mask at a distance of 130 metres. If any light hit the rim of the mask a very prominent echo was obtained. The divergence assessed through a more conventional method, by measuring the diameter of the fluorescing spot on a piece of paper at two distances, gave 0.8 mrad. It is pronbably the Raman shifter which gives rise to this phenomenon. The gas in the Raman cell is heated by the radiation, which causes movements in the gas and temperature gradients, the gas will act as a non-homogeneous optical medium, and cause some of the radiation to deviate from the original beam, hence an increased divergence.

4:4:1:2. Alternating the wavelength on and off

In normal DIAL measurements, e.g. when SO_2 is monitored, the wavelength is alternated between the on and off values using a stepping-motor with an excentric wheel, which moves the arm connected to the dye-laser's grating. This method is too inexact for mercury measurements, due to the resolving power needed. A new method, which

manages to do the tuning on and off well enough, was developed; the apparatus is described in appendix A. A piezo-electric crystal passes on a movement to the grating arm, which allows a tuning of the dye-laser of 0.5 Å in the wavelength region of interest, 2536.5 Å. This method has proved to keep the settings of the on and off wavelengths very stable, which is an advantage, since the wavelengths may be chosen very close to each other. In this way the phase-matching in the KDP-crystal is retained during the alternation. Since a dispersive element is used in the set-up, slightly different directions of the on and off wavelenghts are expected but corresponding to a wavelength difference of 0.3 Å, the difference in direction will be no more than 40 μrad, and hence negligible. Temperature effects, though, become evident, at least during the first hour of operation, since a change in temperature makes the metallic parts of the device either expand or contract. During this time several wavelength calibrations may be necessary. This is the subject of the next section.

4:4:1:3 Wavelength calibration

First a calibration of the dye-laser's wavelength scale is needed. This is done with a hollowcathode lamp and the optogalvanic effect. As the wavelength is changed an electric circuit indicates when it coincides with a spectral line of neon. When a number of such lines have been obtained a calibration is possible. To find the exact mercury wavelength at 253.65 nm a beam-splitter makes two beams out of the original one, and the intensities are measured by photodiodes. (See Fig.12) A cell containing mercury vapour is introduced into the path of one of the beams, and as the wavelength is successively is changed and the piezo-crystal swept over its full range the correct wavelength is found, sooner or later. (Fig. 15) From this chart appropriate values for on and off wavelengths may be computed. As can be seen, none of the structures in the absorption line appears as in Fig. 1, the linewidth of the laser is too great.

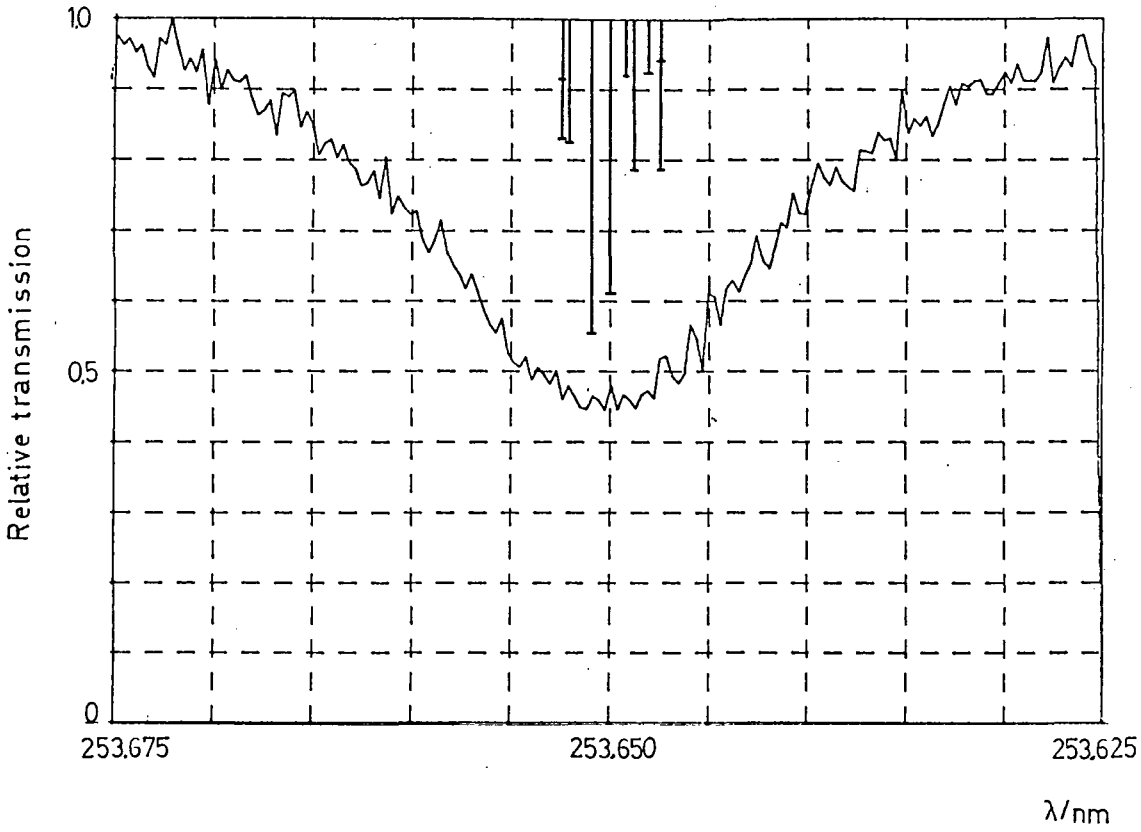

Fig. 15 Calibration recording, obtained through comparing the intensities of two beams, one of which one has passed through a 25 mm cell of mercury vapour, and by sweeping the dye-laser with the piezo tuning device. The structure of the mercury transition is also shown.

4:4:2. Initial measurements

With the set-up described in previous sections, some initial measurements were made. The range achievable with the system, which of course in lidar contexts is an interesting parameter, was investigated. In order to verify that a plume of mercury vapour really could be detected, DIAL measurements were made in which the laser beam was directed through a chamber containing mercury vapour. Further tests are being planned, employing an absorption cell, which should keep the mercury vapour inside for a longer period of time, permitting longer measurement times to be used.

4:4:2:1. Range measurements

The range achievable is an interesting system property. In the measurements made the wavelength was alternated between the on and off values, calibrated for mercury. The output pulse energy was 0.5 mJ and the transient recorder was set to detection intervals of 10 ns, corresponding to a length of 1.5 m. An example of a raw recorded signal, smoothed with a gaussian profile with a half-width of 10 channels, is presented in Fig. 16.

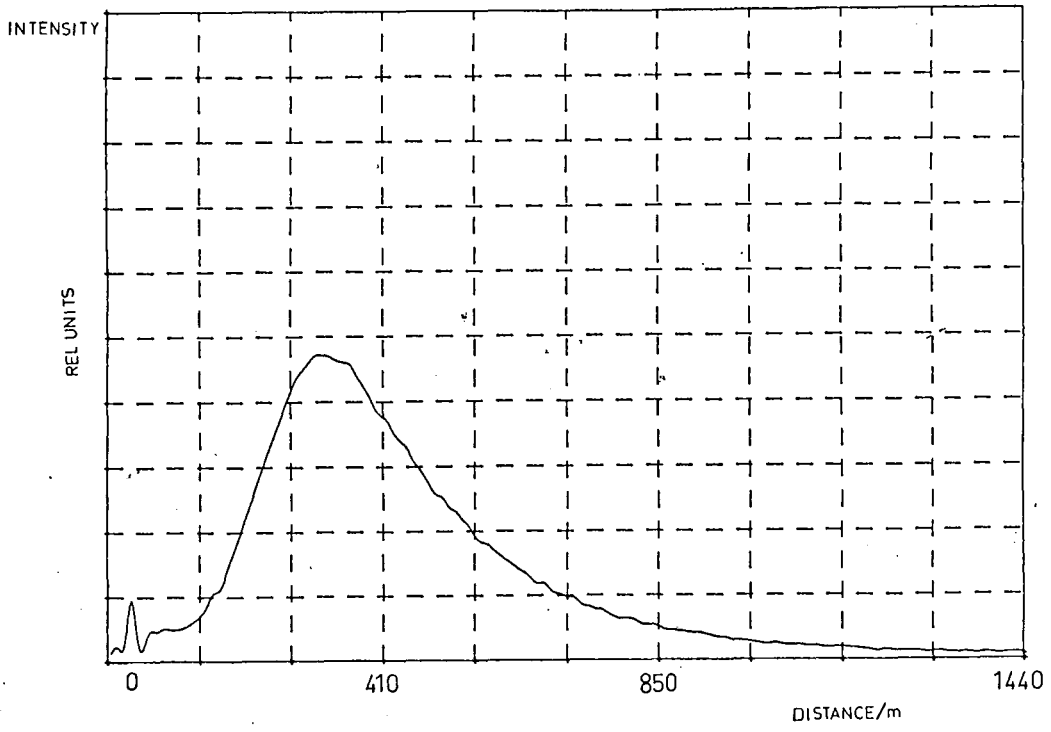

Fig. 16 Raw recorded lidar signal. Average of 200 shots.

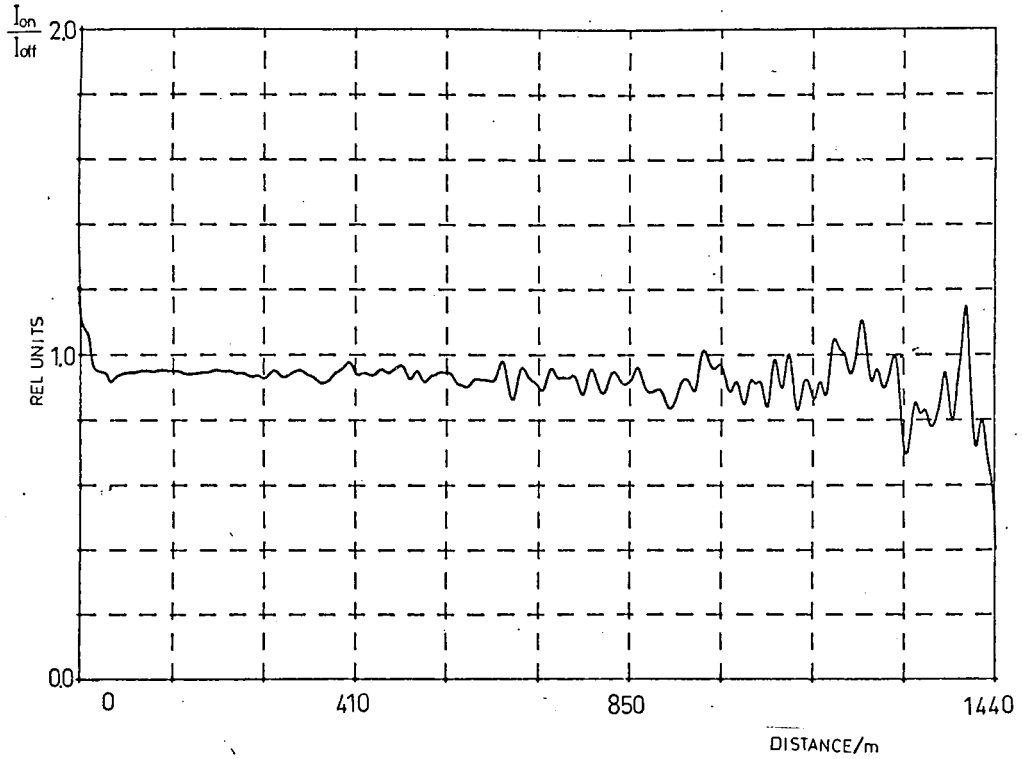

Fig. 17 DIAL curve for a 40s measurement (25 cycles, 1 cycle=8 shots on, 8 shots off).

The measurement time was 40 s (25 cycles, 1 cycle= 8 shots on, 8 shots off, and one recording when the laser light is blocked).
A DIAL curve with the on and off signals divided, for a 25 cycle measurement, is shown in Fig. 17. By extending the time of measurement the signal-to-noise ratio may be improved, and hence the range increased. Notice the small, but significant slope of the DIAL curve in Fig. 17. This slope indicates that mercury is present in the atmosphere, it is caused by the background concentration.

The DIAL curves may sometimes differ from the value 1, not considering noise effects but a translation of the curves upwards or downwards. This is due to the positioning of the on and off wavelengths. If they are not adjusted symmetrically around the wavelength value which gives optimum phase-matching in the KDP crystal, the output energies will not be equal.

4:4:2:2. DIAL measurement of mercury vapour in a chamber

A cylindrical chamber, with a diameter of 45 cm and a length of 180 cm, was used at a distance of 130 m from the system. A vessel with liquid mercury was put inside the chamber, proving a mercury vapour pressure as

the openings of the chamber were closed. The temperature was about 14 ^{0}C and the chamber was kept closed for 2-4 minutes before a measurement, in order to get enough vapour in the chamber. It was quite windy, which caused the vapour to disappear quickly as the chamber was opened. The recordings were made with an output pulse energy of 0.4 mJ. Some results are presented in Figs.18-21.

Fig.18 shows the raw recording of the on and off signals of a 3-cycle measurement. The peak at 130 m, where the beam passes the chamber, is caused by resonance fluorescence by the mercury atoms. This peak remains after division by the off signal, and will therefore also appear in the DIAL curve. The step downwards in DIAL curves at 130 m is caused by the mercury vapour. The curves shown in Fig. 19 and Fig. 20 are two consecutive measurements, each 1 cycle, corresponding to a measurement time of 1s. It is clearly seen how the mercury concentration decreases with time as the wind empties the chamber of vapour.

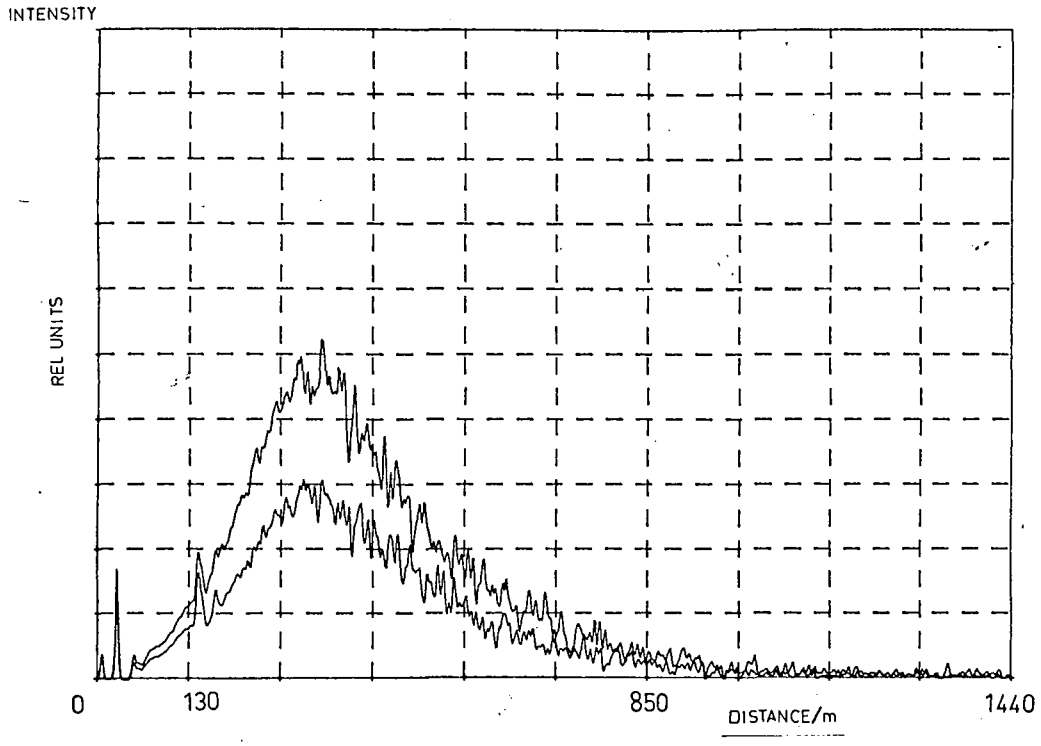

Fig. 18 Recordings of the on and off signals (3 cycles). The chamber is located at 130 m. The lower curve is the on signal.

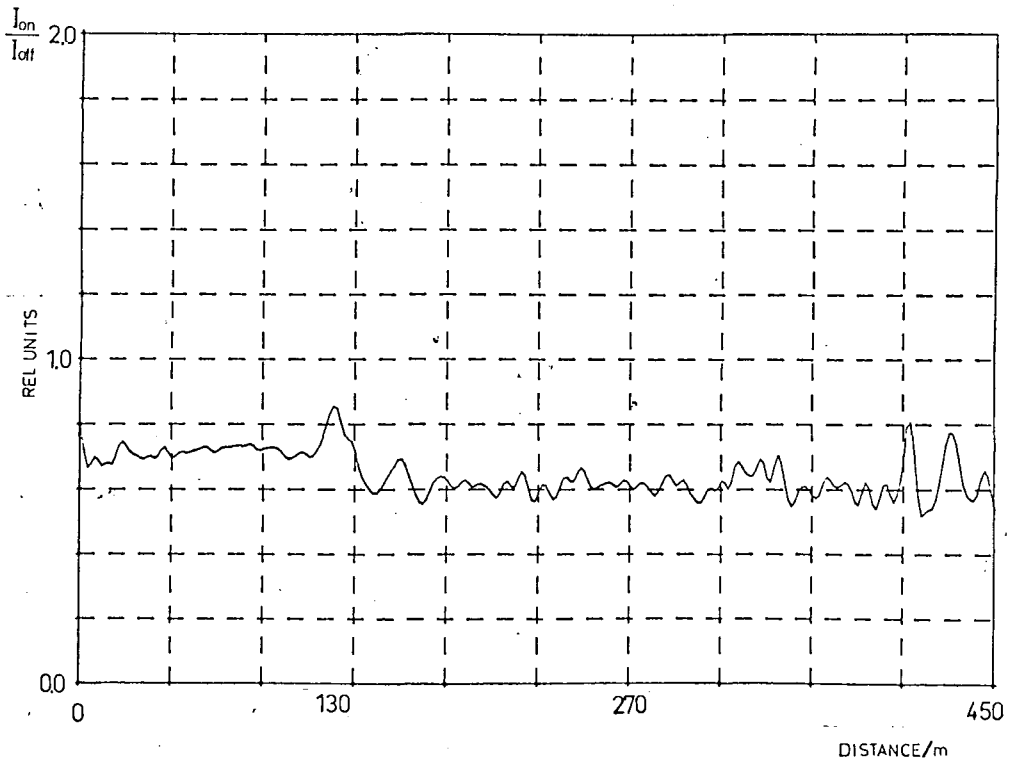

Fig. 19 DIAL curve for a 3-cycle measurement through the chamber.

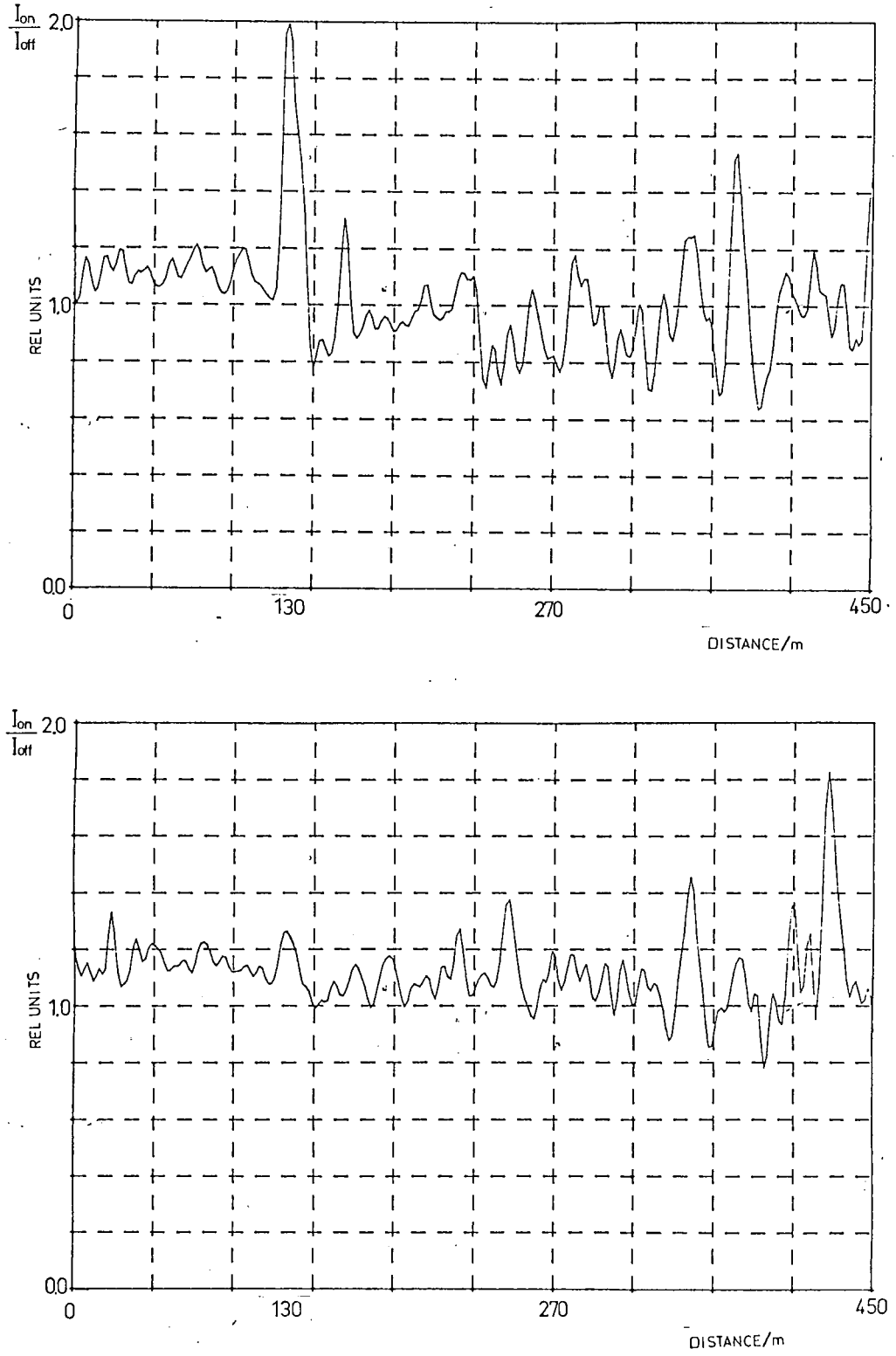

Fig. 20 DIAL curves for two consecutive 1-cycle measurements, separated by about 1 second.

4:4:3. Discussion

As proved in these initial measurements, monitoring of atmospheric mercury is possible with the DIAL technique. Some questions, though, remain. For instance, if resonance fluorescence affects the measurements. The fluorescence causes some of the light which has been absorbed by mercury atoms to reach the detector (see Fig.18), which of cource introduces an error. The effect of this phenomenon has to be further investigated.

Fluorescence was also recorded for the off wavelength. Since the mercury atoms ought not to absorb at this wavelength, this is puzzling and has also to be further investigated.

Considering the sensitivity of the system, different applications have to be treated separately. If only an averaged value is desired, it is sufficient to record the absorption from one point to another. Then there is no need for any range resolution, and the DIAL curve may be smoothed heavily, which will eliminate some of the noise. As shown in the range measurements, for a 25-cycle measurement, the range limit for such a recording is at least 1.5 km, and with an estimated cross-section of 5.10^{-19} m^2, the detection limit will be of the order of 1 ppt (part per trillion, =8.2 ng/m^3), corresponding to an overall absorption of 2 %. DOAS measurements made in Lund [11], showed that the concentration of mercury in this city was of the order of 2.5 ppt, which should be detectable with the lidar system. In the measurements made, e.g. the one showed in Fig.17, the absorption over a path of 1.3 km is 4%, which leads to a mercury concentration of 2-3 ppt, clearly in parity with the DOAS measurements.

When making range-resolved measurements the analysis becomes more complex. The sensitivity varies with range, the signal-to-noise ratio decreases with range due signal fall off, and the degree of range resolution desired. Table 1 gives the estimated optical density which should give an absorption of the order of the noise level for the measurement shown in Fig.17. The measurement time was 40s (25 cycles) and the DIAL curve has been smoothed to a degree which gives a maximum range resolution power of 50 m.

Further tests employing the absorption cell described in appendix B, will be made in order to determine system parameters and optimize the range and the sensitivity of the system. Other methods of generating the laser light will also be examined.

Another lidar approach, gas correlation lidar, (see [18]), will be investigated, and its performance when applied to atmospheric mercury monitoring will be tested.

Table 1: Estimated sensitivity for a 40s measurement with a resolution power of 50 m.

Range	optical density of Hg/(ppbm)
0 - 200 m	1.5
200 - 400 m	5
400 - 600 m	10
600 - 800 m	20
800 - 1000m	40

Appendix A. Construction of a piezo-electric tuning system

The piezo crystal is a Physic-Instrumente P-255 and has a range of 27 µm. The device is steered by the computer which through necessary interfaces and a D/A-converter controls a Physic-Instrumente P-263 voltage supply, which delivers a voltage (0 - -1500 V) to the crystal.

The crystal is built into a conventional micrometer shaft and mounted on a steel plate, which replaces the dye laser's push-plate. Three different positions of the micrometer shaft on the steel plate are possible, corresponding to different settings of the dye laser. (in order to have the crystal as perpendicular as possible to the wavelength arm, to avoid friction and doubtful movements).

The capacity of the crystal is large, 8nF, which makes the cut-off frequency low (around 20 Hz). The repetition rate of the YAG-laser, though, is only 10 Hz, and the crystal has proved to work well.

Fig. 21 shows a photograph of the device, and the circuitry for the D/A converter is shown in Fig. 22.

Fig. 21 Photograph of the micrometer shaft with the piezo crystal and the steel-plate.

A/D converter unit

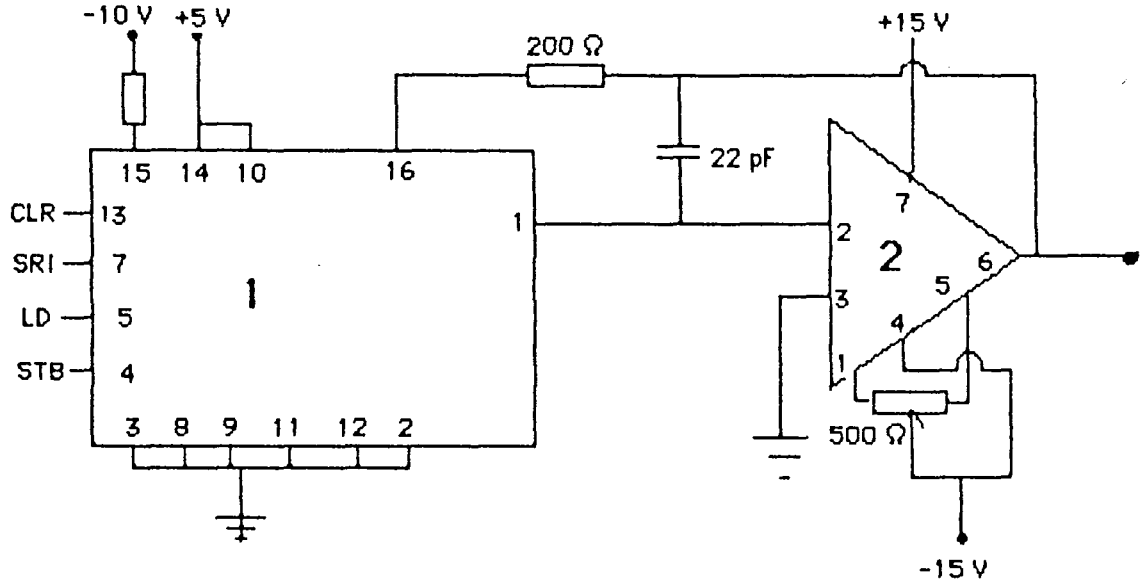

1.. Analog devices AD 7543 JN

2. µA 741

Voltage supply

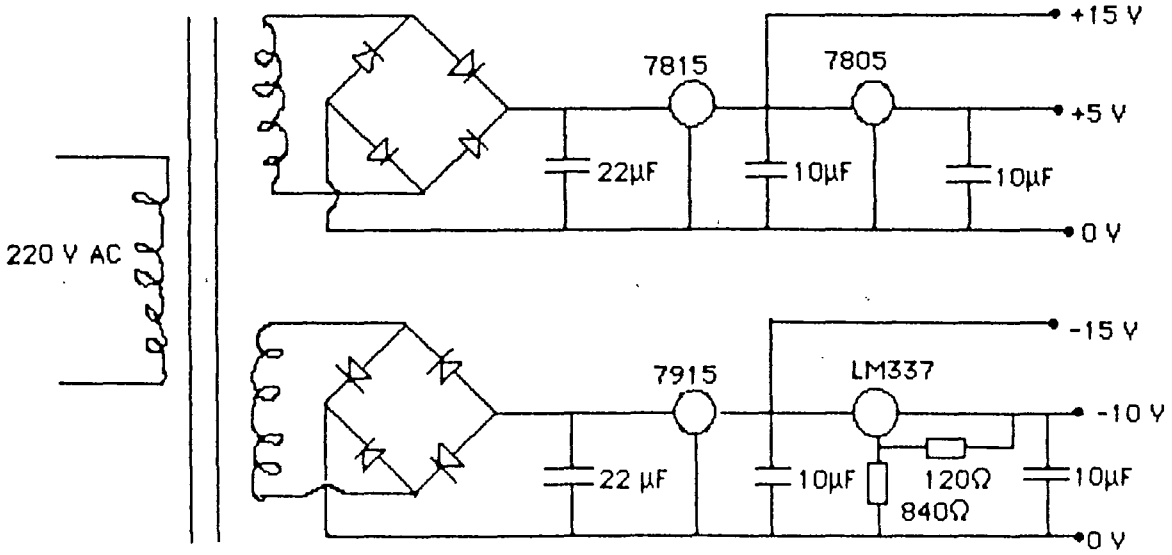

Fig. 22 Circuitry for the D/A converter unit.

Appendix B. Construction of an absorption cell

In order to obtain a convenient method of testing the lidar system, an absorption cell was constructed. The difficulties with previously used chambers have been the tendency of the vapour to disappear too quickly. This difficulty has been partly overcome with this cell construction, by increasing the volume. A method of opening the chamber which allows for quick openings, and synchronizing it with the start of the measurement has also been considered important, since as long measurement time as possible is desired.

The cell is assembled in sections, each with a length of 1 m, and with a cross-section of 80*80 cm. The sections are constructed with a frame of standard aluminium profiles and aluminium plates. Any number of sections may be used, in order to obtain a suitable length for the application under investigation. The surface inside the chamber has been covered with a layer of a protective material, preventing the aluminium from being contaminated when reactive chemicals, like mercury, are used. Fans on the cell floor keep the gas inside in motion, which may be necessary when heavy elements are used. Each section is equipped with an adjustable leg.

The ends consists of three distinguishable parts with different functions. (Fig. 23) Part 1 is a frame of aluminium profiles making up the main and supporting part of the gable. Part 2 is the door construction, which consists of two aluminium plates sliding on a rail of aluminium. Part 3 is a mask with a circular hole, defining the size of the opening. The doors are pulled by springs towards the position when the cell is open. Closing the cell is achieved by pulling a string which is connected to both the doors.